An Analytical Model for Predicting Forming/Switching Time in Conductive-Bridge Resistive Random-Access Memory (CBRAM)

Shaoli Lv, Jun Liu, Lingling Sun
Key Laboratory of RF Circuits and Systems (designated by Ministry of Education in China), Hangzhou Dianzi University, Hangzhou 310037, China

He Wang, Jinyu Zhang†, and Zhiping Yu
Institute of Microelectronics, Tsinghua University, Beijing 100084, China
†corresponding author: zhangjinyu@tsinghua.edu.cn

Abstract—Analytical solutions (i.e., compact model) to differential equations governing the surface movement of conductive filament (CF) in CBRAM have been developed. Time needed for forming and switching of memory cell can readily be evaluated based on the device structure and the applied bias. The accuracy of the model has been verified by comparison to both experimental and numerical simulation results for Ag-GeS_2-W CBRAM cells.

Keywords—CBRAM; filament growth; cation migration

I. Introduction

With its fast switching speed and ease in fabrication, conductive-bridge resistive random-access memory (CBRAM) stands out as one of promising candidates for resistive-switching RAMs (RRAMs) [1][2]. For future circuits design a compact model of CBRAM becomes necessary.

It becomes critical to predict the forming/switching time in a quick manner for optimization of cell structures and design of biasing conditions. The switching of CBRAM is generally attributed to the formation and rupture of metallic conductive filaments (CFs) in the solid electrolyte within the memory cell, and differential equations (DEs) for governing CF growth/rupture have been proposed in [3], which are usually solved through numerical simulation. In this paper, we have developed analytical solutions to these DEs, leading to the fast evaluation of the cell performance in terms of forming/switching times.

II. Analytical Model

The forming process in CBRAM consists of 1) atom ionization (in our case it is Ag) at the anode under positive bias (with respect to the cathode); 2) ion (Ag^+) migration towards the anode driven by the applied electric field; 3) reduction of ions at the cathode to become atoms (Ag), especially around some micro-bumps pre-existed on the cathode, where the electric field is large; 4) growth of this metallic filament with sharp tip toward the anode until the filament touching the anode. This forming process has been simulated numerically in our previous work [4]. In order to develop an analytical model for forming/switching time, we simplify the above picture to electrolyte being a conductive plate with conductivity controlled by the applied bias. In Fig. 1, it is shown (clockwise) schematically the complete process of forming and switching.

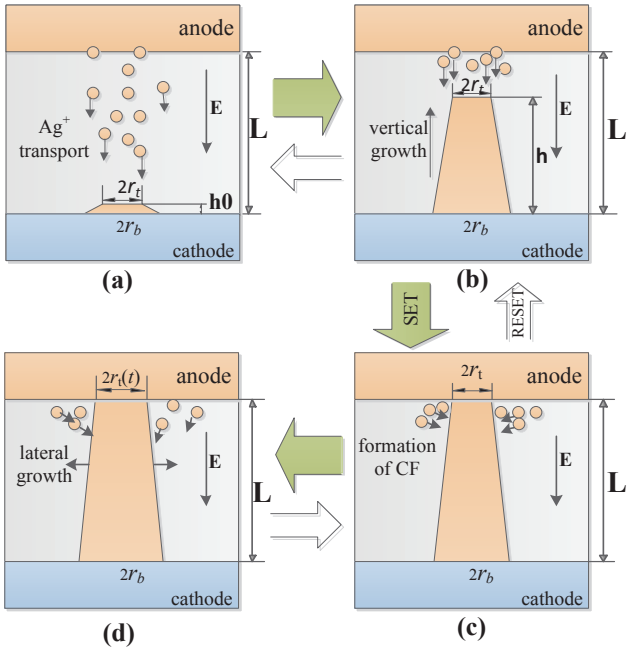

Fig. 1 (a), (b) Filament height growth/shrink (r_t, r_b fixed); (c), (d) Filament width expansion/shrink (h fixed).

The forming process is divided into two stages in this work: first, ionized atoms transport from the anode to cathode under the applied electric field. Second, when ions reach the cathode, the reduction of ion leads filament growth from the cathode to anode which is defined as filament vertical growth here.

Initial Migration of Cations

The transport of cations in the electrolyte is assumed of

The work is sponsored by the National Basic Research Program of China (973 Program #2011CBA00600) and SRC #2224.001 in the U.S.

978-1-4673-5736-4/13/$31.00 ©2013 IEEE

Mott-type [5], and the initial time for cations to migrate from anode to cathode can be evaluated as follows,

$$T_{tran}=\frac{L}{v_m},\ \text{with}\ v_m=\alpha_m f\cdot e^{-\frac{E_m}{kT}}\sinh\left[\frac{q\alpha_m(V-V_0)}{2LkT}\right] \quad (1)$$

where L, v_m, V, V_0 are the thickness of the electrolyte layer, ion migration velocity, the applied voltage, and the work function difference between the anode and cathode, respectively; α_m, f, and E_m are ion hopping distance, frequency, and barrier height, respectively; all other symbols have conventional meaning.

Vertical Growth of CF

When cations reach the cathode, they will be reduced to metal atoms there. And once the filament is formed, this reduction process will also occur at the surface of the metallic filament, leading to the filament growth from the cathode to anode. This filament growth process is much like an electroplating, and the velocity of the metal surface (for both cathode and CF) movement on the normal direction to the surface depends on the normal electric field at the surface. For Mott-type of transport in the electrolyte, which is assumed to have uniform conductivity, this CF growth rate (i.e., the velocity) is determined by the following equation.

$$\frac{dh(t)}{dt}=v_h\cdot e^{-\frac{E_a}{kT}}\cdot\sinh\left[\frac{Zaq(V-V_0)}{2kT(L-h(t))}\right] \quad (2)$$

where, h is the height of the metallic filament, v_h is the hopping velocity, Z is the number of electron charges of the ion, E_a is the activation energy, a is the hopping distance, and V and V_0 are the same as in (1). The key point is that the surface movement rate, dh/dt, has dependence on the normal field $E=(V-V_0)/(L-h)$ in a hyperbolic sine (sinh) function.

the boundary condition for the phase of vertical growth is

$$\mathrm{BC}_1:\ h(0)=h_0,\ h(t_{SET})=L$$

As soon as the tip of the filament reach anode, SET occurs and the device changes from HRS to LRS.

SET time of the device, t_{SET}, can be solved from Eq.(2) and BC_1

$$t_{SET}=2a_0b_0\left(\mathrm{Ei}\left[s(h_0)\right]-\frac{e^{s(h_0)}}{s(h_0)}\right) \quad (3)$$

where, $s(h)=\frac{aqZ|V-V_0|}{2(h-L)kT}$, $a_0=\frac{e^{-E_a/kT}}{v_h}$, $b_0=\frac{aq|V-V_0|Z}{2kT}$, $\mathrm{Ei}(\lambda)=\int_{-\infty}^{\lambda}e^{\xi}/\xi\,d\xi$ is the exponential integral, h_0 is set to 0 at SET condition.

In [3], Eq.(2) is solved through numerical simulation. However, in this work, instead of numerical integration, analytical formulas are found for t as function of h, an inverse function of $h(t)$, in this work.

$$t(h)=t_{SET}-2a_0b_0\left(\mathrm{Ei}\left[s(h)\right]-\frac{\mathrm{e}^{s(h)}}{s(h)}\right) \quad (4)$$

The key step in finding the analytical solution to Eq.(2) is the realization that for large argument x in $\sinh(x)$, the function behaves just like $\exp(x)$, hence the use of exponential integral $\mathrm{Ei}(x)$ in our analytical solution.

Lateral Growth of CF

Cations continue to be reduced around the filament after SET if the positive bias is still applied. This leads to the lateral growth of the filament. The lateral process is also dominated by a differential equation shown below

$$\frac{dr_t(t)}{dt}=v_r\cdot e^{-\frac{E_a}{k(T+V^2R_{th}/R_L)}}\cdot\sinh\left[\frac{\beta q(V-V_0)}{k(T+V^2R_{th}/R_L)}\right] \quad (5)$$

where v_r is the lateral growth rate, R_{th} is the thermal resistance in units K/W, and R_L is the resistance of cell in LRS.

Analytical expression of the filament radius during the lateral growth as solved from Eq. (5) is as follows,

$$r_t(t)=\frac{b_1-c_1\left[\mathrm{e}^{a_1(t-t_{SET})}-1\right]}{d_1} \quad (6)$$

where,

$a_1=\mathrm{e}^{-\frac{\pi r_t r_b E_a}{x}}v_r x\left[-2\beta I_{cc}L\rho\pi q r_b T\cdot\cosh(y)-2E_a I_{cc}^2L\rho\pi r_b R_{th}\cdot\sinh(y)\right]$,

$b_1=\beta I_{cc}L\rho\pi q r_t r_b T\cdot\cosh(y)+E_a {I_{cc}}^2L\rho\pi r_t r_b R_{th}\cdot\sinh(y)$,

$c_1=(I_{cc}^4kL^2\rho^2{R_{th}}^2+2I_{cc}^2kL\rho\pi r_t r_b R_{th}T+k\pi^2r_t^2r_b^2T^2)\cdot\sinh(y)$,

$d_1=2I_{cc}L\rho\pi r_0\left[\beta qT\cosh(y)+E_aI_{cc}R_{th}\sinh(y)\right]$,

$x=1/k(I_{cc}^2L\rho R_{th}+\pi r_t r_b T)$, $y=\beta I_{cc}L\rho qx$, r_t is the top radius of the CF before SET.

To get an analytical solution to Eq.(5), the first-order Taylor approximation is used in the solving procedure.

Lateral Dissolution of CF

By applying a negative bias voltage, an inverse process would happen. 1) Metal atoms in the filament are oxidized to ions; 2) The ions moves toward anode under applied negative electric field; 3) ions get reduced at anode. The dissolution process also has two stages: lateral dissolution and vertical dissolution. The formed filament first tends to laterally dissolve, radius of the CF shrinks as in Eq.(7)

$$r_t(t)=\frac{b_2-c_2\cdot(e^{a_2t}-1)}{d_2} \quad (7)$$

where,

$$a_2 = \frac{2e^{-\frac{E_a L\rho}{kx_1}} L\rho\pi r_b R_{th}(V-V_0)^2 v_r \left[E_a \sinh(y_1) - \beta qV\cosh(y_1)\right]}{kx_1^2},$$

$$b_2 = \left[\beta qV^3\cosh(y_1) - 2E_a\sinh(y_1)\right] L\rho\pi r_{tm} r_b R_{th}(V-V_0)^2,$$

$$c_2 = kx_1^2\sinh(y_1),$$

$$d_2 = L\rho\pi r_b R_{th}(V-V_0)^2\left[\beta qV\cosh(y_1) - E_a\sinh(y_1)\right],$$

$$x_1 = LpT + \pi r_{tm}^2 R_{th}(V-V_0)^2, \quad y_1 = \frac{\beta L\rho q(V-V_0)}{kx_1}.$$

the boundary condition for the lateral dissolution is

$$BC_2: \quad r_t(0) = r_{tm},\ r_t(t = t_{RESET}) = 0$$

r_{tm} is initial radius of CF at the start of RESET process.

Once the top radius of the filament shrinks to below r_t, we consider the filament detached from the anode at which time RESET occurs, the device changes from LRS back to HRS.

RESET time of the device is solved from Eq. (7)

$$t_{RESET} = -e^{\frac{E_a L\rho}{kx_1}} kx_1^2 \frac{\ln\left[\frac{\sqrt{kx_1^2 + 2\beta L\rho\pi q r_{tm}^2 R_{th}(V-V_0)^3\coth(y_1)} - 2E_a L\rho\pi r_{tm}^2 R_{th}(V-V_0)^2}{\sqrt{kx_1^2}}\right]}{L\rho\pi r_{tm} R_{th}(V-V_0)^2 v_r\left[\beta qV\cosh(y_1) - E_a\sinh(y_1)\right]} \tag{8}$$

Vertical Dissolution of the CF

If the applied negative bias still exists after high-resistance state (HRS) occurs during RESET, the metallic filament will be dissolved vertically until completely disappeared. The vertical dissolution of the filament is in contrary to the phase of vertical growth, and can be expressed by t as a function of h. And h is from L to 0.

$$t = t_{RESET} + 2a_0 b_0\left(\mathrm{Ei}[s(h)] - \frac{e^{s(h)}}{s(h)}\right) \tag{9}$$

III. Model Verification

In this part, we verify the results from the analytical model by comparing the analytical solutions with the numerical simulation and the experimental results in order to confirm the validity of the analytical expressions.

In Fig. 2, results are shown from the analytic solutions and numerical simulation to differential equation (1), which dominates the vertical growth, at different applied bias, and it can be seen that they are almost exactly the same.

Analytical solution and numerical solution to differential equation (2), which dominates the lateral growth, are plotted in Fig.3 with different applied bias. Again, it can be seen that the two types of solutions are almost identical.

The model prediction of the forming time for a Ag-GeS_2-W CBRAM with various electrolyte film thickness has been compared to experimental data [6] as shown in Fig.4.

Table 1 Parameters used in the compact model

Parameters	Value	Parameters	Value
E_m	0.57eV	v_r	700m/s
f	10^{13}Hz	I_{cc}	5μA
a_m	10nm	r_b	180nm
E_a	0.4eV	r_t	110nm
v_h	20m/s	β	0.35
a	2.5nm	R_{th}	10^5K/W
V_0	0.6V	Z	1

The total forming time is the sum of T_{tran} and t_{SET} which are defined in Eqs. (1) and (3), respectively. The calculated results are obtained using the same set of parameters except of different thickness of GeS_2 layer. Good agreement has been achieved for three thicknesses for electrolyte layer of 12, 20, 40nm. Both experimental and calculation results indicate that forming time vs. applied voltage is determined by two different slopes in semi-logarithmic behavior. At high voltage, the well-known exponential behavior of forming time [7] is captured. At low voltage, the exponential behavior that dominates filament growth is limited by the ion migration velocity, which exponentially depends on the applied voltage. From low to high applied voltage, the forming operation switches from ion-migration limited to chemical-reaction limited.

IV. Discussion

The analytical model for CBRAM given in this paper considers both the memory cell structure and biasing condition. The model reveals the following switching principles: First, the set voltage should be larger than the work

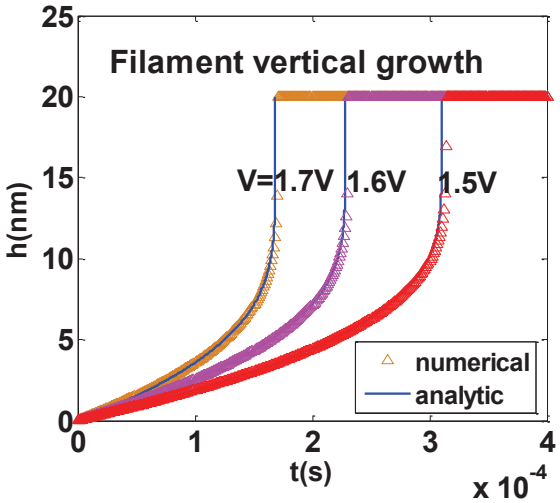

Fig. 2 Comparison between analytical and numerical solutions in filament vertical growth for different applied voltages during the SET process with L=20nm.

function difference between the electrodes for anode and cathode, otherwise there would be no effective voltage drop across the function layer of electrolyte. Second, large applied voltage leads to a short switching time of a CBRAM cell. Ion migration time across the electrolyte layer is a critical factor in the overall forming or switching time. Ion migration velocity through the solid electrolyte is closely related to the applied voltage amplitude. Thus the applied voltage amplitude could significantly alter the forming or switching time. Based on this analytical model, we can calculate an optimal forming or switching voltage once the cell structure is determined. Or vice versa, from the desired forming/switching time, we can design an optimal cell structure for the CBRAM.

And through the comparison with the experimental data, we also verified that from low to high applied bias voltages for different film thickness the limiting factor may change from ion-migration limited to chemical-reaction limited.

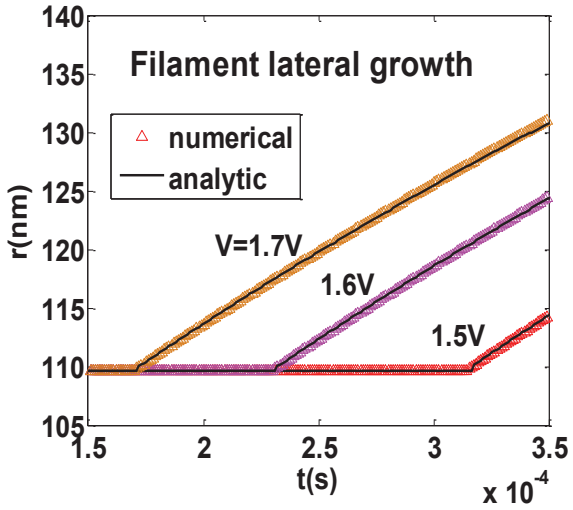

Fig. 3 Comparison between analytical and numerical solutions in filament lateral growth for different applied voltages during the SET process

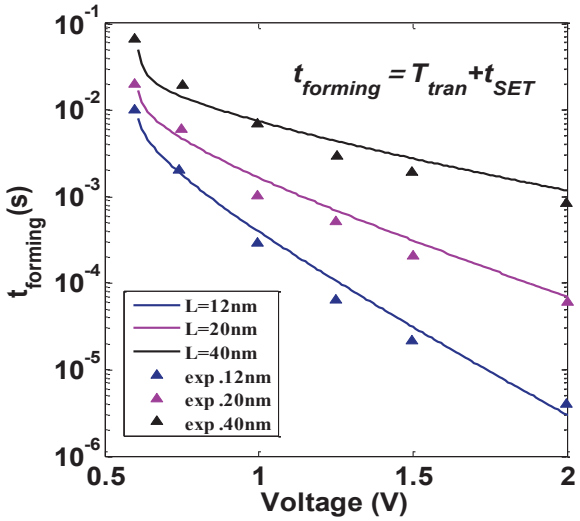

Fig.4 Comparison between analytical solution and experimental data in the forming process.

V. Conclusion

A physics-based analytical model for CBRAM forming and switching has been developed. The good agreement with the experimental data proves the accuracy of the model and its scalability. The advantage of such a compact model is that it allows the fast evaluation of cell/biasing design and can be further implemented in SPICE simulation for RRAM circuits.

References

[1] W. Otsuka, *et al*., "A 4Mb conductive-bridge resistive memory with 2.3GB/s read-throughput and 216MB/s program throughput". *ISSCC*, 2011, pp. 210-211.

[2] Kund, M, *et al.,* "Conductive bridging RAM (CBRAM): an emerging non-volatile memory technology scalable to sub 20nm". *IEEE International Electron Devices Meeting, IEDM Technical Digest*, 2005, pp.754-757.

[3] Shimeng, Y, *et al.,* "Compact Modeling of Conducting-Bridge Random-Access Memory (CBRAM).", *IEEE Transactions on Electron Devices,* 2011, 58(5), pp.1352-1360.

[4] Sen, L, *et al.,* "Electrochemical simulation of filament growth and dissolution in conductive-bridging RAM (CBRAM) with cylindrical coordinates". *IEEE International Electron Devices Meeting (IEDM)*, 2012, pp.26.3.1-26.3.4.

[5] N. F. Mott and R. W. Gurney, *Electronic Processes in Ionic Crystals*. London, U.K.: Oxford Univ. Press, 1948.

[6] Jameson, J. R, *et al.*, "Effects of cooperative ionic motion on programming kinetics of conductive-bridge memory cells". *Applied Physics Letters,* 2012, 100(2), pp. 023505-023505-4.

[7] Russo, U, *et al.* "Study of Multilevel Programming in Programmable Metallization Cell (PMC) Memory". *IEEE Transactions on Electron Devices*, 2009, 56(5), pp. 1040-1047.